



Radiation Sources and their Application for Beam Profile Diagnostics

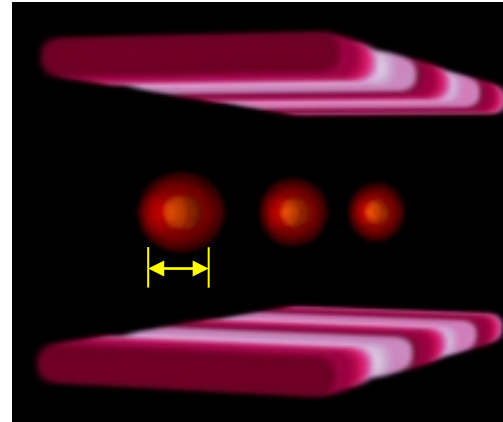
Gero Kube
DESY / MDI
gero.kube@desy.de

- Introduction to Imaging
- Transverse Profile Measurements based on OTR and ODR
- Parametric X-Ray Radiation
- Coherent Radiation Diagnostics and Smith-Purcell Radiation

Size Measurements

task

- › determination of beam profile
 - measurement of characteristical size (rms, ...)



courtesy:
J. Amundson (FNAL)

conventional size measurement

- › take object and measure



difficulties

- › object extremely small
- › object not directly accessible
 - inside vacuum beam pipe, accelerator environment, ...

optical imaging

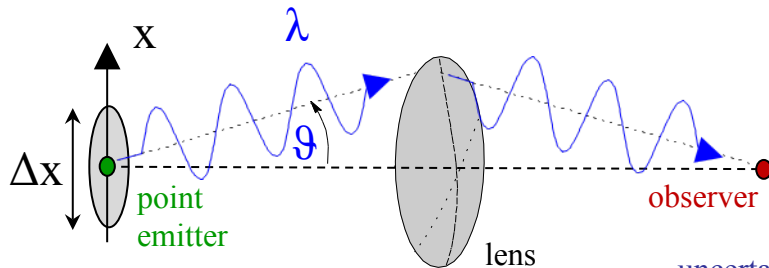
- › generate replica in comfortable environment
- › adjust replica size (image) to size of measuring device (CCD)

Imaging and Resolution

- neglect lens imperfections (aberrations)
- diffraction limited systems → high quality, aberration-free systems

fundamental resolution limit

- point observer detecting photons from point emitter → location of emission point ?



$$\Delta p_x = 2\hbar k \cdot \sin \theta \approx 2 \cdot \frac{h}{2\pi} \cdot \frac{2\pi}{\lambda} \cdot \sin \theta$$

$NA = \sin \theta$:
numerical aperture

uncertainty principle: $\Delta x \cdot \Delta p_x \approx h \Rightarrow$

$$\Delta x \approx \frac{\lambda}{2 \sin \theta}$$

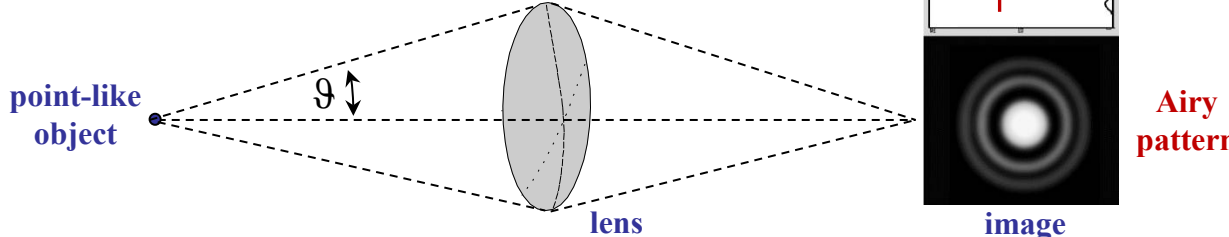


high resolution:

(i) small λ

(ii) high NA

image of point source



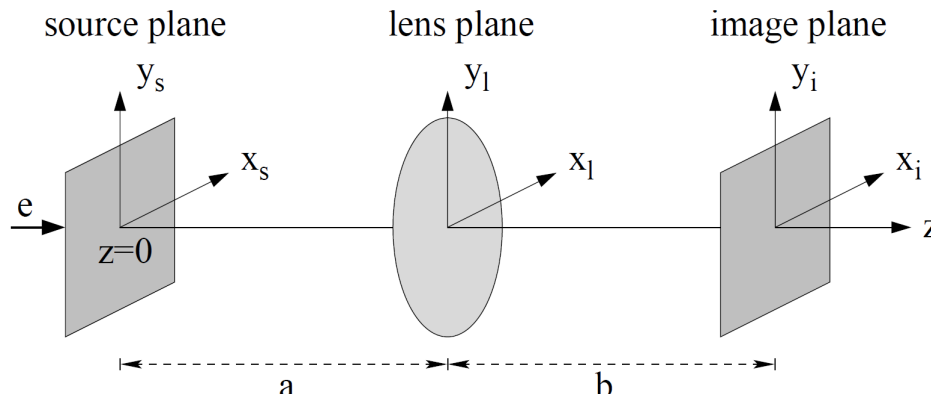
<http://www.astro.ljmu.ac.uk>

$$\Delta x = 0.61 \frac{M\lambda}{\sin \theta}$$

magnification M

Fundamentals of Image Formation

- detailed resolution information
 - requires basic knowledge of image formation
- simple imaging setup



- procedure
 - calculate image of point source (single particle radiation) → **Point Spread Function (PSF)**
 - image of extended object → 2-dim. convolution of **source distribution** and PSF
 - resolution → difference between source distribution and image (resp. PSF)
- PSF calculation
 - el. field in source plane
 - field propagation from element to element → in frame of scalar diffraction theory
 - (i) source plane – lens input
 - (ii) lens input – lens output
 - (iii) lens output – image plane
 - intensity distribution in the image plane

Fundamentals of Image Formation

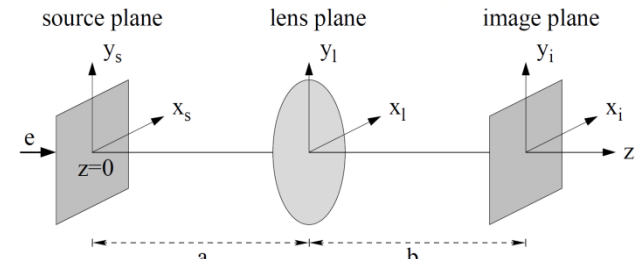
- source field

- radiation field → depends on mechanism of radiation generation

- propagation

- scalar diffraction theory

(here: from source to lens plane)



$$E_{x_l, y_l}^l(\vec{r}_l, \omega) = -i \frac{e^{ika}}{\lambda a} \cdot e^{i \frac{k}{2a} (x_l^2 + y_l^2)} \int_{-\infty}^{+\infty} \int_{-\infty}^{+\infty} dx_s dy_s E_{x_s, y_s}^s(\vec{r}_s, \omega) \cdot e^{i \frac{k}{2a} (x_s^2 + y_s^2)} \cdot e^{-ik \frac{x_s x_l + y_s y_l}{a}}$$

aperture boundaries

- far field (Fraunhofer) approximation: $\frac{k}{2} (x_s^2 + y_s^2)_{\max} \ll a$

$$\rightarrow E_{x_l, y_l}^m(\vec{r}_l, \omega) = -i \frac{e^{ika}}{\lambda a} \cdot e^{i \frac{k}{2a} (x_l^2 + y_l^2)} \int_{-\infty}^{+\infty} \int_{-\infty}^{+\infty} dx_s dy_s E_{x_s, y_s}^s(\vec{r}_s, \omega) \cdot e^{-i(k_x x_s + k_y y_s)} \propto \mathcal{F}(E_{x_s, y_s}^s) \quad \left(k_{x,y} = k \frac{x_s, y_s}{a} \right)$$

→ basis of Fourier Optics

- thin lens approximation

- quadratic phase shift: $E_{x_l, y_l}^{l_{out}}(\vec{r}_l, \omega) = E_{x_l, y_l}^{l_{in}}(\vec{r}_l, \omega) \cdot e^{-i \frac{k}{2f} (x_l^2 + y_l^2)}$

with $\frac{1}{f} = \frac{1}{a} + \frac{1}{b}$

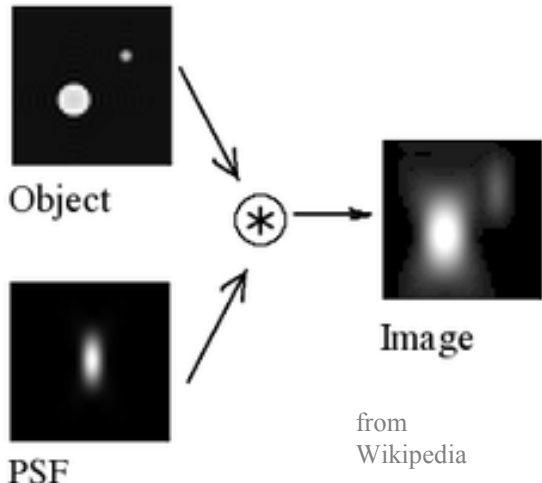
- intensity

$$\frac{d^2 W}{d\omega d\Omega} = \frac{c}{4\pi^2} \left(|\vec{E}_{x_i}^i(\vec{r}_i, \omega)|^2 + |\vec{E}_{y_i}^i(\vec{r}_i, \omega)|^2 \right)$$

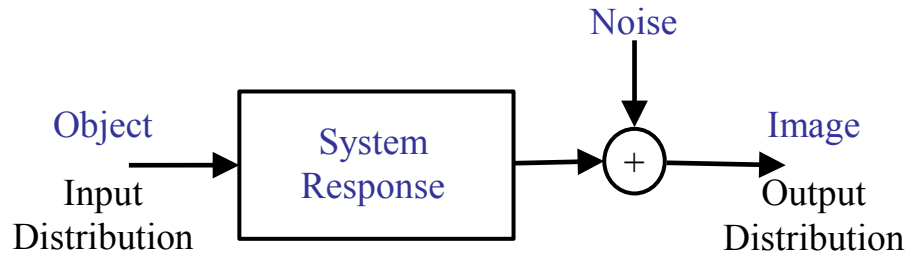
Image Formation: Systems Approach

• image formation

$$\text{Image} = \text{PSF} \otimes \text{Object} + \text{Noise}$$



• systems approach to imaging (Fourier Optics)



‣ Point Spread Function (PSF)

- image of a point source (single particle)
- characteristic of the imaging instrument
- deterministic function

‣ noise

- nondeterministic function
- described in terms of statistical distributions

‣ „standard“ signal theory

- 1-dim. signals (in time domain)
- system analysis with **delta pulse**

‣ imaging

- 2-dim. signals (in spatial domain)
- system analysis with **point source**
system response: **PSF**

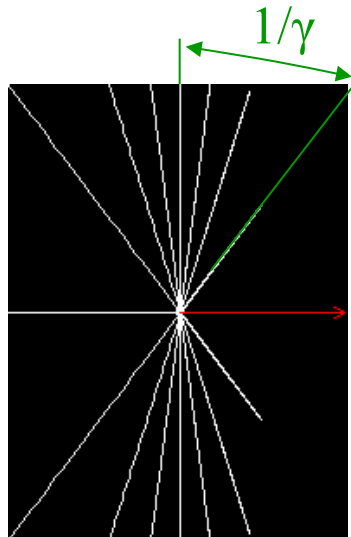
Radiation Generation: Considerations

radiation generation via particle interaction with matter

- ▶ luminescent screen monitors

radiation generation via particle electromagnetic field

- ▶ particle electromagnetic field
- ▶ relativistic contraction characterized by Lorentz factor



electric field lines
in LAB frame

$$\gamma = E / m_0 c^2$$

E : total energy

$m_0 c^2$: rest mass energy

proton: $m_p c^2 = 938.272 \text{ MeV}$

electron: $m_e c^2 = 0.511 \text{ MeV}$

$\gamma \rightarrow \infty$: plane wave

- ▶ $mc^2 = 0 \text{ MeV}$:

- ▶ ultra relativistic energies :

light \rightarrow „real photon“

idealization \rightarrow „virtual photon“

Separation of Particle Field

- electromagnetic field bound to particle observation in far field (large distances)
- separation mechanisms

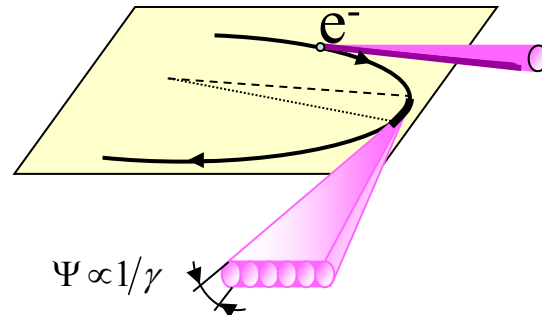
- bending of particle via magnetic field
- synchrotron radiation
- circular accelerators



linear accelerators: no particle bending !

}

separate field from particle



- diffraction/reflection of particle electromagnetic field via material structures

exploit analogy between real/virtual photons:

- light reflection/refraction at surface ↔ backward/forward transition radiation (TR) ↗
- light diffraction at edges ↔ diffraction radiation (DR) ↗
- light diffraction at grating ↔ Smith-Purcell radiation ↗
- light (X-ray) diffraction in crystal ↔ parametric X-ray radiation (PXR) ... ↗

Synchrotron Radiation

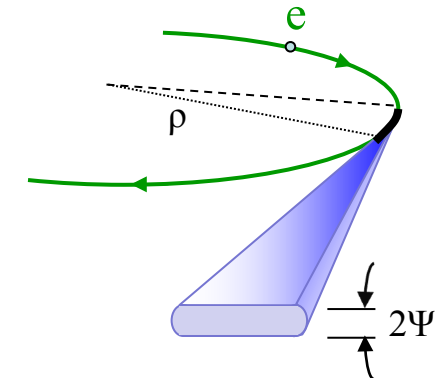
- circular accelerator: radiation source available for free

‣ bending magnet (wiggler, undulator)

- non-invasive

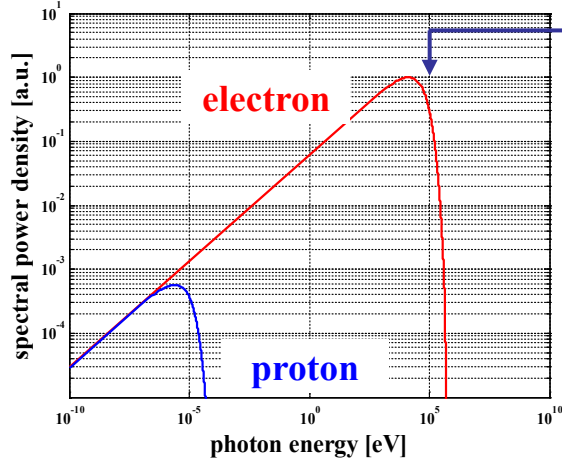
- strong collimation (vertical)

‣ opening angle: $\Psi \propto 1/\gamma$



- emission over wide spectral range

‣ choice of operational range



g : Lorentz factor

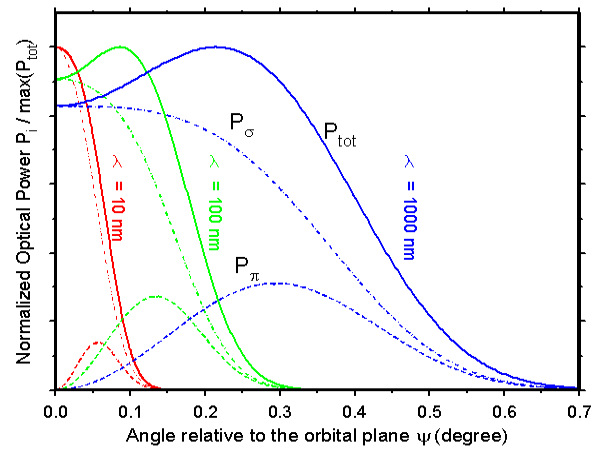
r : bending radius

$E_{kin} = 20 \text{ GeV}$

$\rho = 370 \text{ m}$

- polarized

‣ define vertical angular divergence



- particle beam diagnostics: resolution

‣ electric field propagation through optical elements

→ radiation field

SR Field: Standard Text Book

- source field: particle field described by **Liénard-Wiechert potentials**:

$$\varphi(t) = \left(\frac{-e}{R(1 - \hat{n} \cdot \vec{\beta})} \right)_\tau, \quad \vec{A}(t) = \left(\frac{-e \vec{\beta}}{R(1 - \hat{n} \cdot \vec{\beta})} \right)_\tau$$

► field derivation: $E(t) = -\vec{\nabla} \varphi(t) - \frac{1}{c} \dot{\vec{A}}(t), \quad \vec{H}(t) = \vec{\nabla} \times \vec{A}(t)$

$$\rightarrow \vec{E}(t) = -e \left(\frac{(1 - \beta^2)(\hat{n} - \vec{\beta})}{R^2(1 - \hat{n} \cdot \vec{\beta})^3} + \frac{\hat{n} \times [(\hat{n} - \vec{\beta}) \times \dot{\vec{\beta}}]}{cR(1 - \hat{n} \cdot \vec{\beta})^3} \right)_\tau, \quad \vec{H}(t) = \hat{n} \times \vec{E}(t)$$

neglect velocity term (far field approximation)

- Fourier transform:

$$\vec{E}(\omega) \approx -\frac{i\omega e}{cR} \int_{-\infty}^{+\infty} d\tau [\hat{n} \times [\hat{n} \times \vec{\beta}]] e^{i\omega(\tau + R(\tau)/c)}$$

- special case: charged particle moving on circular orbit

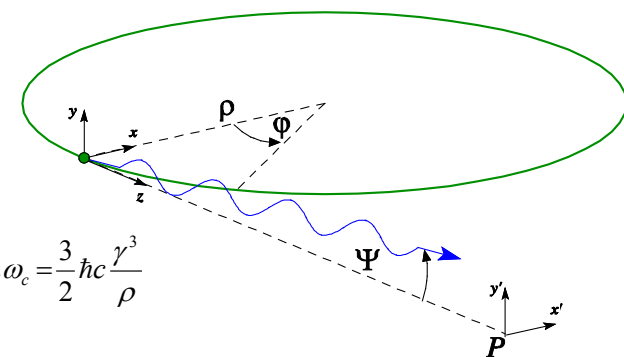
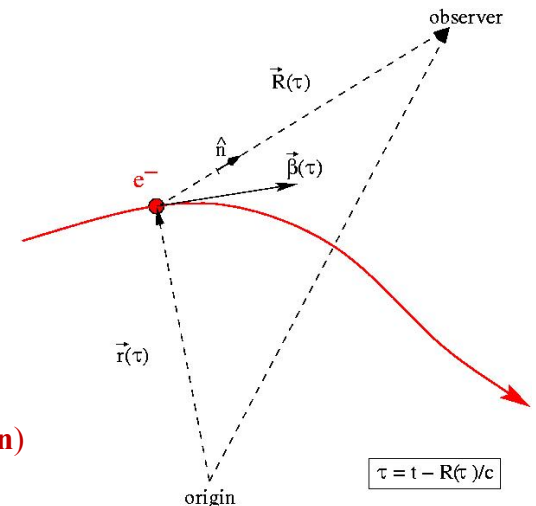
$$E_x(\omega) = E_\sigma = A_\sigma \frac{\hbar\omega}{2\hbar\omega_c} (1 + \gamma^2 \Psi^2) \cdot K_{2/3} \left[\frac{\hbar\omega}{2\hbar\omega_c} (1 + \gamma^2 \Psi^2)^{3/2} \right]$$

$$E_y(\omega) = E_\pi = A_\pi \frac{\hbar\omega}{2\hbar\omega_c} \gamma \Psi \sqrt{1 + \gamma^2 \Psi^2} \cdot K_{1/3} \left[\frac{\hbar\omega}{2\hbar\omega_c} (1 + \gamma^2 \Psi^2)^{3/2} \right]$$

$$\text{with } \hbar\omega_c = \frac{3}{2} \hbar c \frac{\gamma^3}{\rho}$$

► analytical field description

- comments:
 - approximative field description → far field approximation
 - emission from single point on orbit → additional contributions: depth of field, orbit curvature



Synchrotron Radiation Field

- second representation: starting point again **Liénard-Wiechert potentials**

$$\varphi(t) = \left(\frac{-e}{R(1 - \hat{n} \cdot \vec{\beta})} \right)_\tau, \quad \vec{A}(t) = \left(\frac{-e \vec{\beta}}{R(1 - \hat{n} \cdot \vec{\beta})} \right)_\tau$$

- Fourier transform of potentials:

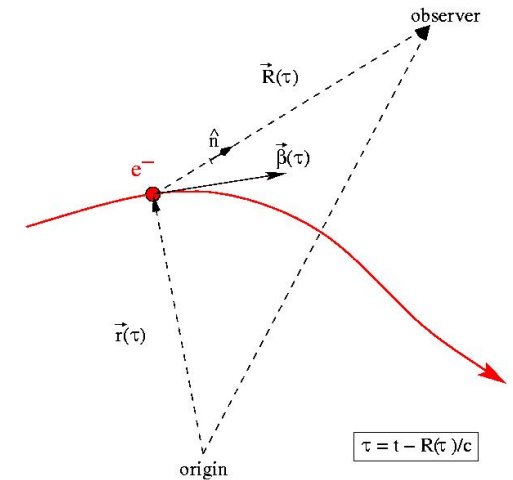
$$\varphi(\omega) = -e \int_{-\infty}^{+\infty} d\tau \frac{1}{R(\tau)} e^{i\omega(\tau+R(\tau)/c)}, \quad \vec{A}(\omega) = -e \int_{-\infty}^{+\infty} d\tau \frac{\vec{\beta}(\tau)}{R(\tau)} e^{i\omega(\tau+R(\tau)/c)}$$

- field derivation:

$$\vec{E}(\omega) = -\frac{i\omega e}{c} \int_{-\infty}^{+\infty} d\tau \left[\frac{(\vec{\beta} - \hat{n})}{R(\tau)} - \frac{ic}{\omega} \frac{\hat{n}}{R^2(\tau)} \right] e^{i\omega(\tau+R(\tau)/c)}$$

with $\tau = \int_0^z \frac{dz}{c\beta_z(z)} = \frac{1}{c} \int_0^z dz \left[1 + \frac{1 + (\gamma\beta_x)^2 + (\gamma\beta_y)^2}{2\gamma^2} \right]$

O.Chubar and P.Elleaume,
Proc. EPAC96, Stockholm (1996) 1177



- knowledge of arbitrary particle orbit: $\vec{E}(\omega)$ determined
- arbitrary magnetic field configuration: determines orbit and $\vec{E}(\omega)$

- comments:
 - (i) exact field description → numerical near field calculation
 - (ii) includes depth of field & curvature → no additional contributions, only field propagation
 - (iii) free codes available → easy field calculation, even field propagation!

SRW: <http://www.esrf.eu/Accelerators/Groups/InsertionDevices/Software/SRW>

(Chubar & Elleaume, ESRF)

Spectra: <http://radian.rimma.riken.go.jp//spectra/index.html>

(Tanaka & Kitamura, SPring8)

Light Sources: Emittance Diagnostics

• emittance

typical values $\epsilon_x = 1\text{-}5 \text{ nm}\cdot\text{rad}$ and 1% emittance coupling

› example: $s_{\text{hor}} = 40 \text{ mm}$, $s_{\text{vert}} = 20 \text{ mm}$ (PETRA III @ DESY)

fundamental resolution limit (uncertainty principle)

$$\Delta\sigma \approx \frac{\lambda}{2\Delta\Psi}$$

optical imaging: $l = 500 \text{ nm}$ and $D\Psi \approx 1.7 \text{ mrad}$ $Ds_{\text{vert}} = 145 \text{ mm}$

diffraction limited

• X-ray imaging: focusing optics

› reflective optics

Kirkpatrick-Baez mirrors,...

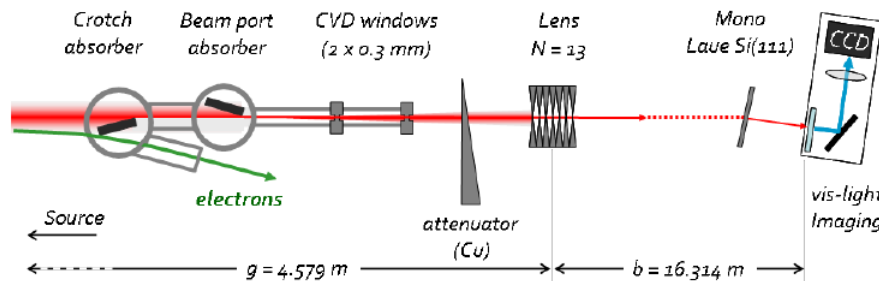
› diffractive optics

Fresnel zone plates,...

› refractive optics

Compound Refractive Lenses (CRL)

CRL monitor @ ESRF (32 keV)



F. Ewald et al., Proc. IBIC 2013, Oxford, UK (2013) 833

• X-ray imaging: non-focusing optics

› pinhole camera

example: Diamond Light Source

C. Thomas et al., Phys. Rev. ST Accel. Beams **13** (2010) 022805

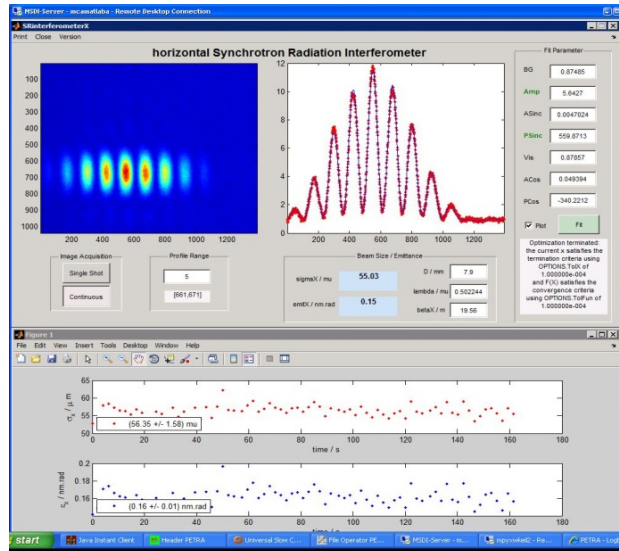
Light Sources: Emittance Diagnostics

SR interferometer

T. Mitsuhashi, Proc. of BIW 2004 Knoxville, Tennessee, p.3

USR studies at PETRA III (DESY):

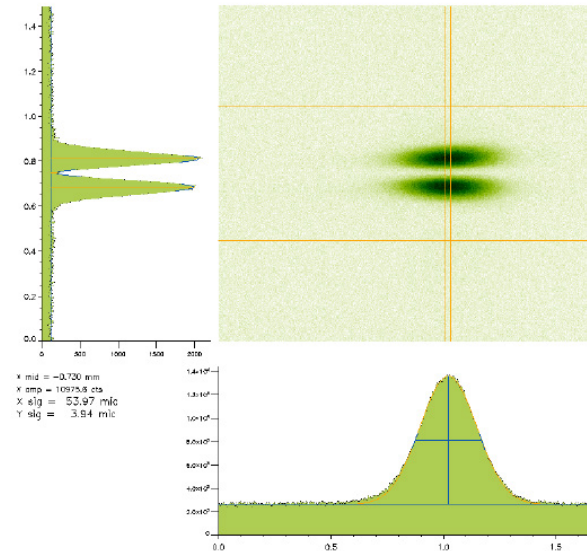
$$\varepsilon_x = 160 \text{ pm.rad} @ 3 \text{ GeV}$$



π -polarisation imaging

V. Schlott et al., Proc. IBIC 2013, Oxford, UK (2013) 519

widely applied @ SLS



coded aperture imaging

R.H. Dicke, Astrophys. Journal 153, L101, (1968)

J.W. Flanagan et al., Proc. DIPAC 2011, Hamburg, Germany (2011) 561

C. Bloomer, „Coded Aperture @ DLS“, TUCZB2

Constant Linear Motion

source field

- point charge with **constant** velocity v → Liénard-Wiechert fields

$$\rightarrow \vec{E}(t) = -e \left(\frac{(1-\beta^2)(\hat{n} - \vec{\beta})}{R^2 (1 - \hat{n} \cdot \vec{\beta})^3} + \frac{\hat{n} \times [(\hat{n} - \vec{\beta}) \times \vec{\beta}]}{cR (1 - \hat{n} \cdot \vec{\beta})^3} \right), \quad \vec{H}(t) = \hat{n} \times \vec{E}(t)$$

no acceleration term

- common representation → cylindrical coordinate system

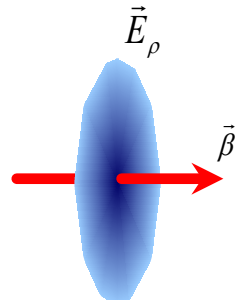
$$\rightarrow \vec{E}(\rho, \varphi, z, \omega) = \frac{e\alpha}{\pi v} e^{i\frac{\omega}{v}z} \left(K_1(\alpha\rho) \hat{e}_\rho - \frac{i}{\gamma} K_0(\alpha\rho) \hat{e}_z \right) \quad \text{with} \quad \alpha = \frac{\omega}{\gamma v} = \frac{2\pi}{\lambda\beta\gamma}$$

- ultra-relativistic particles ($\gamma \gg 1$)

- neglect longitudinal field component
- pure transverse „pancake“ structure
- radial extension: $\alpha\rho \approx 1$

$$\rho = \frac{\lambda\beta\gamma}{2\pi} \approx \gamma\lambda$$

virtual photon range

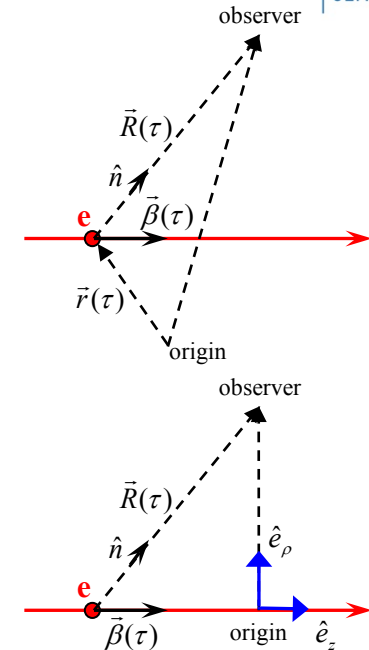


3-dim. theories

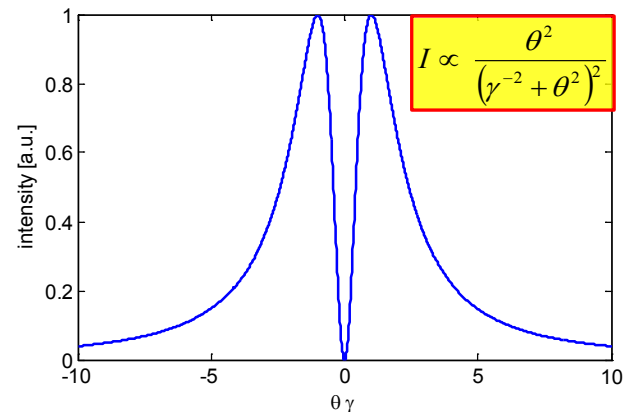
A.G. Shkvarunets and R.B. Fiorito, Phys. Rev. ST Accel. Beams **11** (2008) 012801

D.V. Karlovets and A.P. Potylitsyn, Nucl. Instr. and Meth. **B266** (2008) 3738

- separation of field → different radiation sources

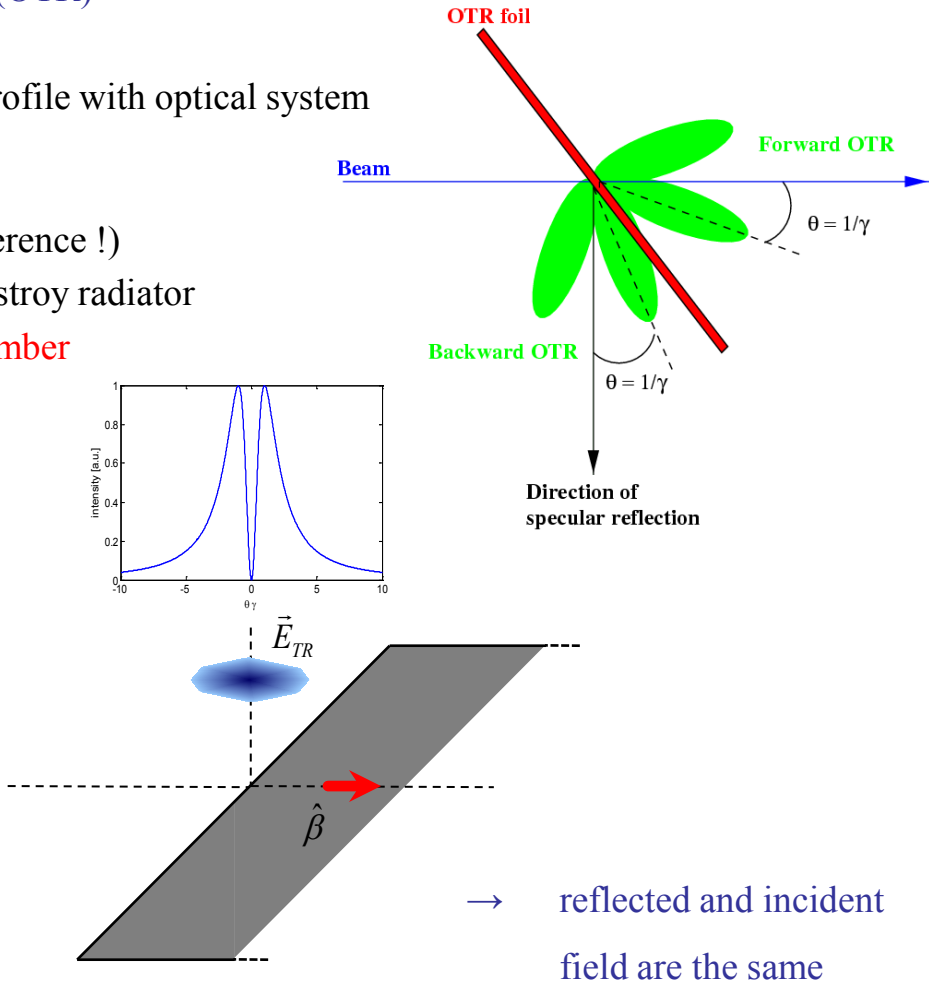
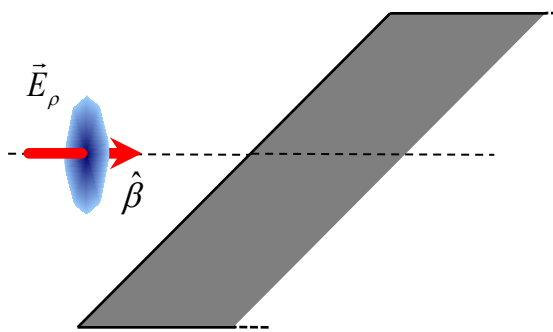


- angular distribution



Transition Radiation

- transition radiation: electromagnetic radiation emitted when a charged particle crosses boundary between two media with different optical properties
- visible part: Optical Transition Radiation (OTR)
- beam diagnostics: backward OTR
 - typical setup: image beam profile with optical system
- advantage: fast single shot measurement
linear response (neglect coherence !)
- disadvantage: high charge densities may destroy radiator
 - limitation on bunch number
- field separation mechanism
 - reflection at boundary (perfect conductivity)



OTR Monitor Resolution

PSF calculation in image plane

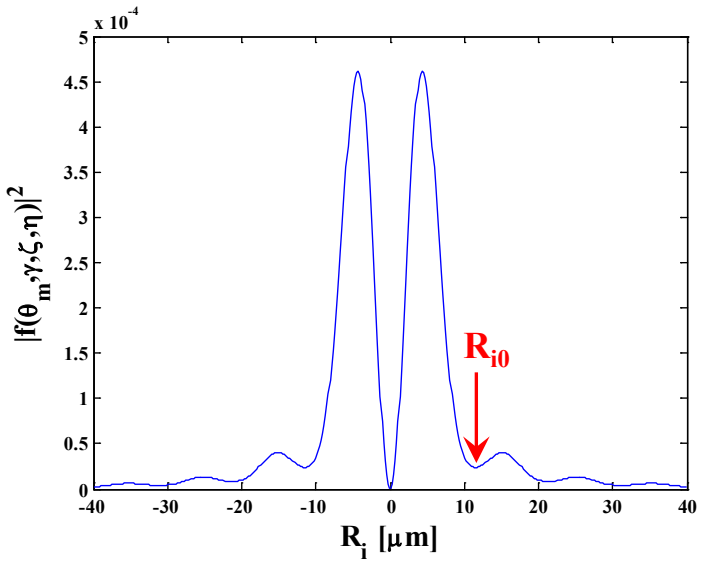
- field propagation in frame of scalar diffraction theory

$$E_{x_l, y_l}^l(\vec{r}_l, \omega) = -i \frac{e^{ika}}{\lambda a} \cdot e^{\frac{i}{2a}(x_l^2 + y_l^2)} \int_{-\infty}^{+\infty} dx_s dy_s E_{x_s, y_s}^s(\vec{r}_s, \omega) \cdot e^{\frac{i}{2a}(x_s^2 + y_s^2)} \cdot e^{-ik\frac{x_s x_l + y_s y_l}{a}}$$

integration limits

- care:** screen dimension \leftrightarrow field extension $\gamma\lambda$
 → might modify radiation properties

OTR resolution for beam imaging (far field)



- resolution definition according to classical optics:

→ first minimum of PSF

(→ diameter of Airy disk)

$$R_{i0} \approx 1.12 \frac{M\lambda}{\theta_m}$$

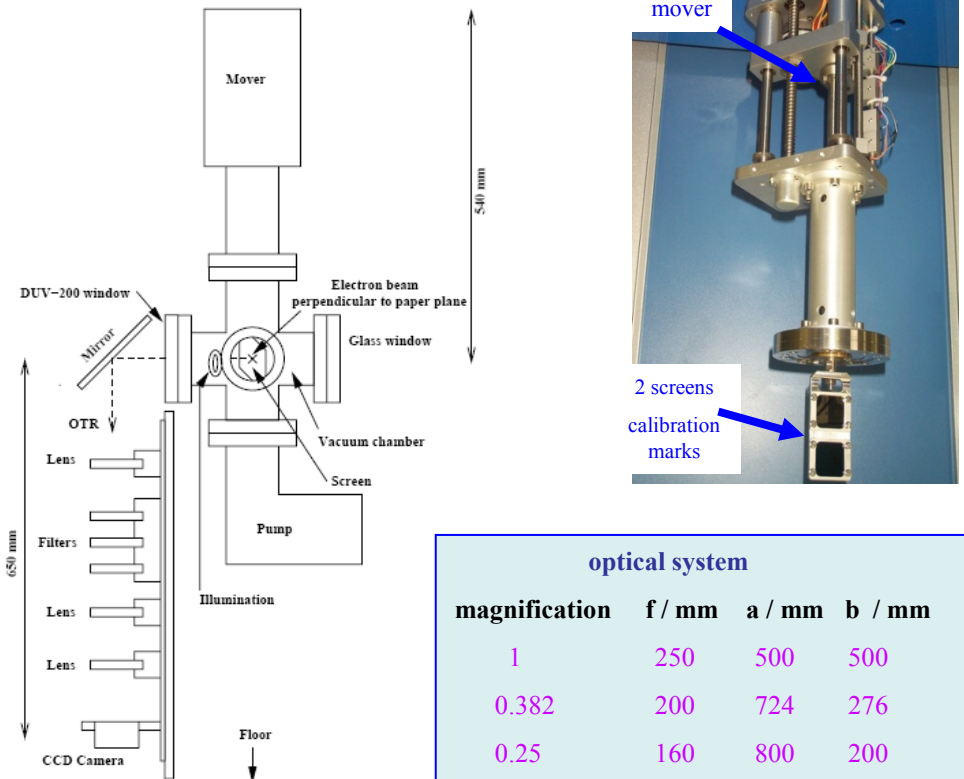
M: magnification

θ_m : lens acceptance angle (NA)

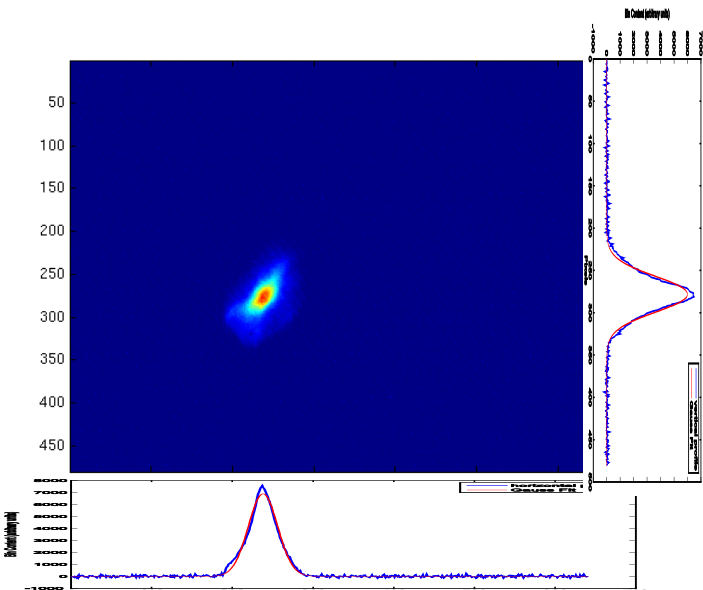
→ θ_m determined by optics, not by radiation properties !

OTR Monitors

- example: FLASH @ DESY



- screen shot: 6 DBC2



K. Honkavaara et al., Proc. PAC 2003, p.2476

- standard monitors @ e-Linacs

▶ 10 keV: R.B. Fiorito et al., Proc. PAC 2007, p.4006

▶ 30 GeV: P. Catravas et al., Proc. PAC 1999, p.2111

- OTR @ hadron accelerators

▶ protons: O.V. Afanasyev et al., Proc. BIW 2006, p.534

V.E. Scarpine et al., Proc. BIW 2006, p.473

▶ heavy ions: B. Walasek-Höhne et al., Proc. HB 2012, p.580

COTR and possible Mitigation

● unexpected Coherent OTR observation during LCLS commissioning

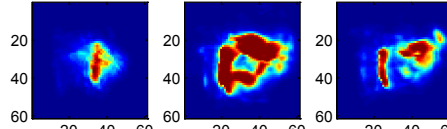
R. Akre et al., Phys. Rev. ST Accel. Beams **11** (2008) 030703

H. Loos et al., Proc. FEL 2008, Gyeongju, Korea, p.485.

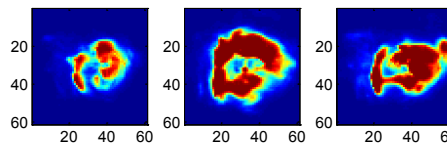
- ▶ strong shot-to-shot fluctuations
- ▶ doughnut structure
- ▶ change of spectral contents



measured spot is no beam image!



courtesy:
H. Loos (SLAC)



● interpretation of coherent formation in terms of "Microbunching Instability"

E.L. Saldin et al., NIM **A483** (2002) 516

Z. Huang and K. Kim, Phys. Rev. ST Accel. Beams **5** (2002) 074401

G. Stupakov, Proc. IPAC 2014, Dresden, Germany (2014), p.2789.

● alternative schemes for transverse profile diagnostics

- ▶ short term perspective: scintillating screen monitors
- ▶ long term perspective: TR imaging at smaller λ

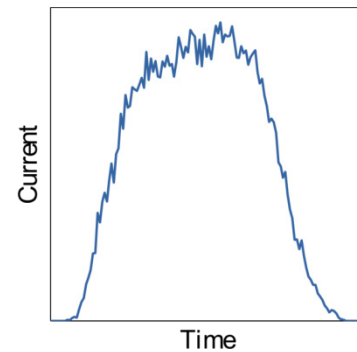
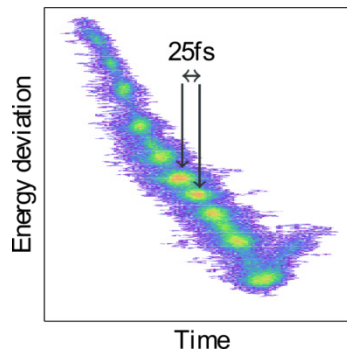
proof of principle experiment @ $\lambda = 19.6$ nm:

L.G. Sukhikh et al., Proc. IPAC 2012, New Orleans (USA), p. 819

and submitted to PRST-AB



additional advantage of better resolution



PSF dominated Imaging

- **image formation**

- standard imaging:

minimize PSF contribution → image is **true replica** of object

$$\text{Image} = \text{PSF} \otimes \text{Object} (+ \text{Noise})$$

- **PSF dominated imaging**

- object size \ll PSF

image dominated by PSF properties

- non-zero object size

→ smearing out of PSF

→ beam size determination
via **image contrast**

- resolution below diffraction limit

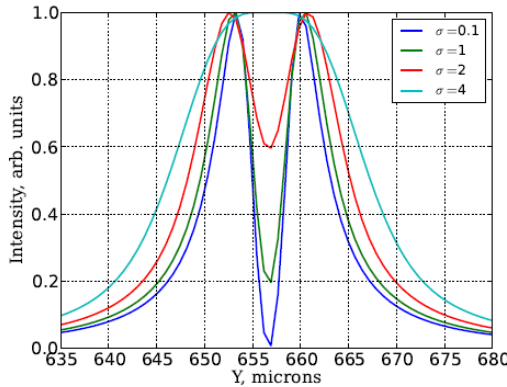
→ resolve sub-micron beam sizes with optical methods

- **experimental verification**

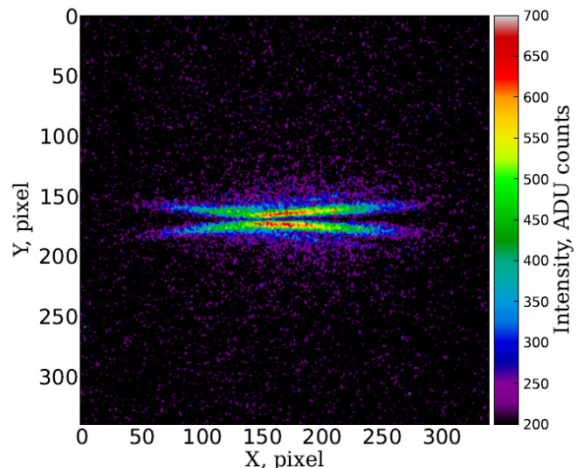
- synchrotron radiation → π -polarisation imaging

- OTR → test experiment @ ATF2

⇒ **minimum measured beam size $(0.754 \pm 0.034) \mu\text{m}$**



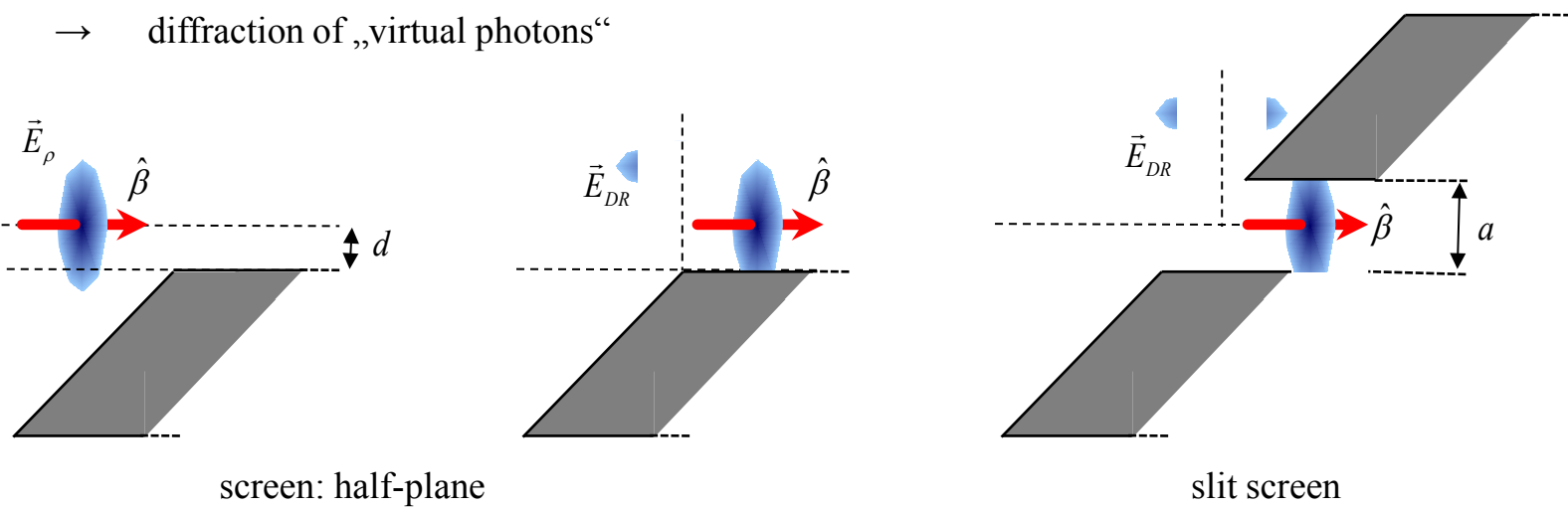
K. Kruchinin et al.,
Proc. IBIC 2013, Oxford, UK, 615
J. Phys.: Conf. Series 517 (2014) 012011



P. Karataev et al., PRL 107 (2011) 174801

Diffraction Radiation

- problem OTR: screen degradation/damage
 - limited to only few bunch operation, no permanent observation
- Optical Diffraction Radiation (ODR): non-intercepting beam diagnostics
 - DR generation via interaction between particle EM field and conducting screen
 - diffraction of „virtual photons“



radial field extension

→ radius $\lambda\beta\gamma / 2\pi \approx \lambda\gamma$

limiting cases

$a \gg \lambda\gamma$: no radiation

$a \approx \lambda\gamma$: DR

$a \ll \lambda\gamma$: TR

- comment: ODR in circular accelerator (CesrTA, Cornell)

L. Bobb et al., Proc. IBIC 2013, Oxford, UK, p. 619

ODR Imaging

PSF calculation in image plane

- field propagation in frame of scalar diffraction theory
 - no beam image, illuminated edge of half-plane

ODR imaging for beam diagnostics

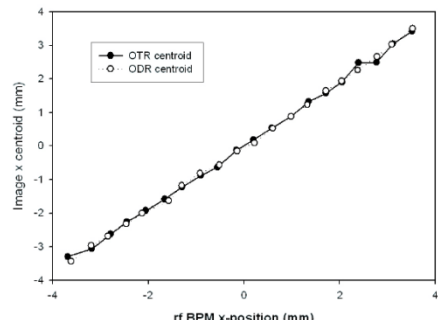
A. Lumpkin et al., Phys. Rev. ST Accel. Beams **10** (2007) 022802

P. Evtushenko et al., Proc. BIW08, WECOTC01 (2008), p.332

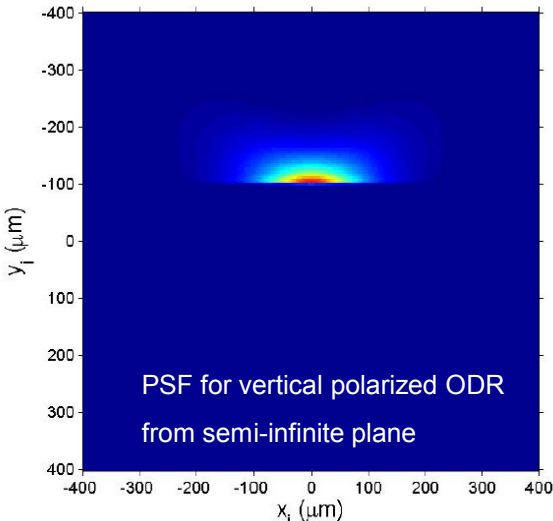
- (relative) 1D beam size monitor: σ_x
 - (i) Gaussian beam profile
 - (ii) known distance between slit edge and beam center
 - pre-defined ROI: projected 1D intensity profile
 - fit profile with Gaussian distribution (σ_x)
 - cross-calibrate σ_x with OTR beam profiles

1D beam position monitor

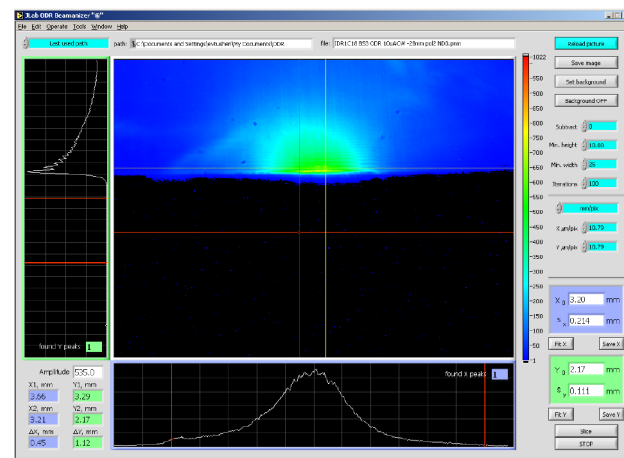
- ODR centroid
- achieved sensitivity: 50-100 μm
($\sigma_x = 1.3 \text{ mm}$, depends on beam size)



D. Xiang et al., Phys. Rev. ST Accel. Beams **10** (2007) 062801



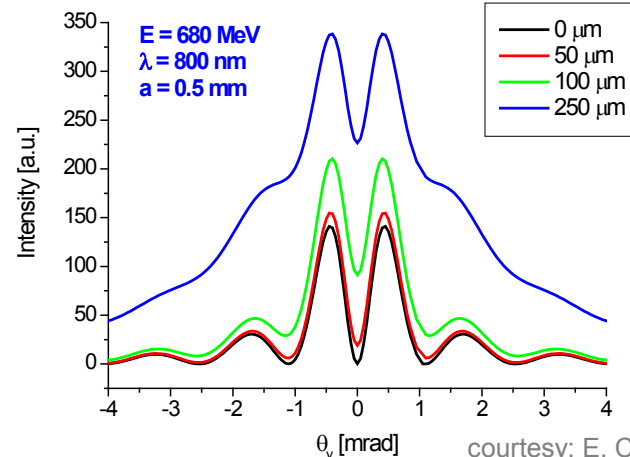
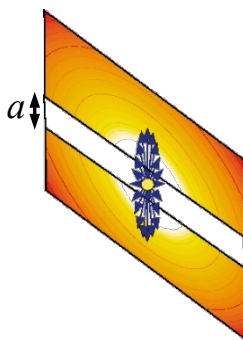
courtesy: P. Evtushenko (JLab)



ODR Angular Distribution

- angular distribution dependence

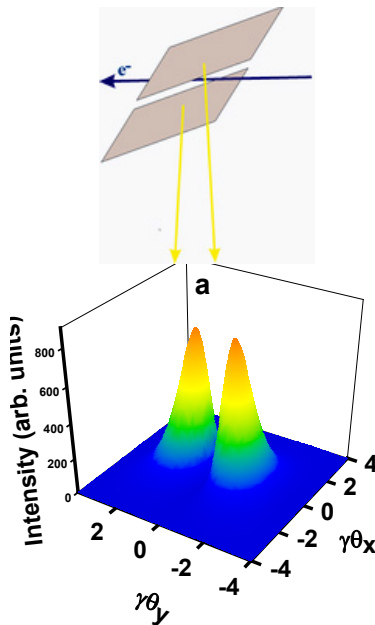
- on beam size
- on beam offset
- beam centered in slit aperture
- on beam divergence x
- interferometric methods



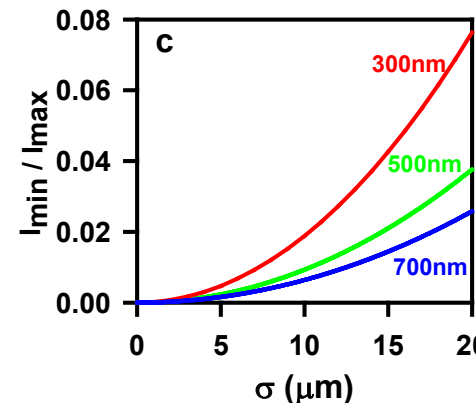
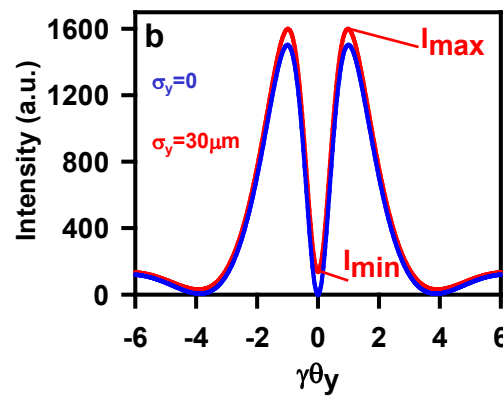
courtesy: E. Chiadroni (INFN)

- 1D beam size determination (σ_y)

P. Karataev et al., Phys. Rev. Lett. **93** (2004) 244802 and Nucl. Instrum. Meth. **B207** (2005) 158



- very low emittance beam ($\epsilon_y = 1.5 \times 10^{-11} \text{ m.rad}$) @ KEK-ATF, centered in slit
- exploit visibility I_{\min} / I_{\max} of projected vertical polarization component



courtesy:
P. Karataev (RHUL)
A. Potylitsyn (TPU)

→ sensitive on beam size $\sigma_y \approx 10 \mu\text{m}$

ODR Interferometry

- beam divergence: DR / ODTR interferometer

R.B. Fiorito and D.W. Rule, NIM **B173** (2001) 167

R.B. Fiorito et al., Phys. Rev. ST Accel. Beams **9** (2006) 052802

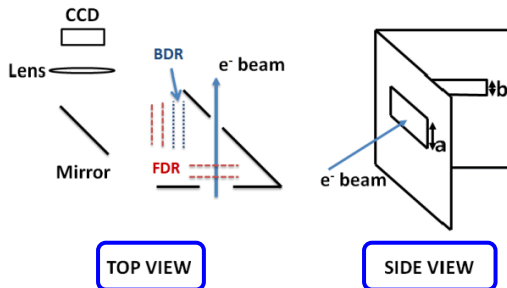
M.A. Holloway et al., Phys. Rev. ST Accel. Beams **11** (2008) 082801

- ODRI: 1D beam size determination @ FLASH (DESY) (separation of beam size, divergence and offset)

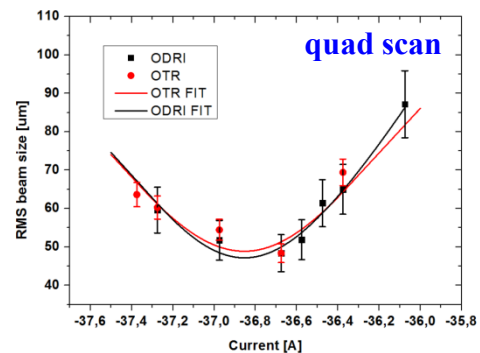
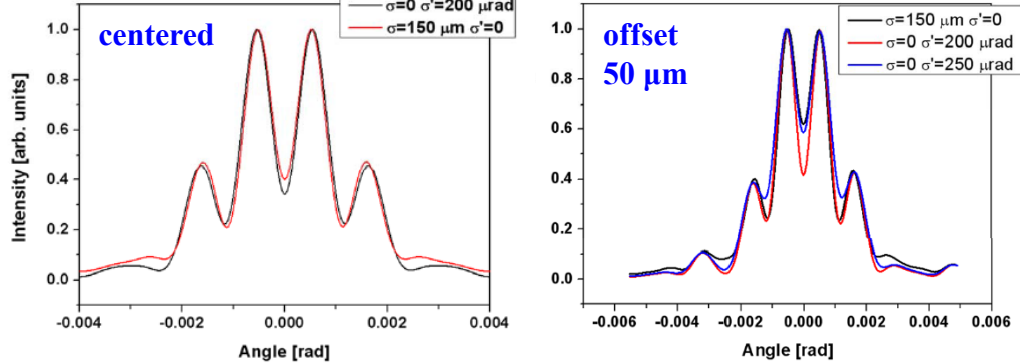
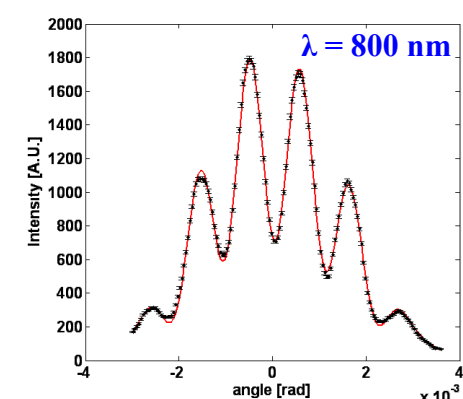
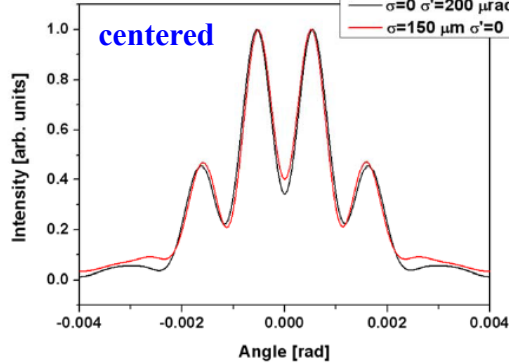
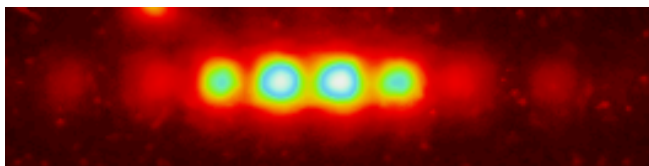
A. Cianchi et al., Phys. Rev. ST Accel. Beams **14** (2011) 102803 and Proc. IPAC 2012, New Orleans, USA, p. 831

- compact double slit arrangement
- both slits with different sizes

second slit within radiation formation length of first one



- σ_y , σ_y' and offset by complex fit routine

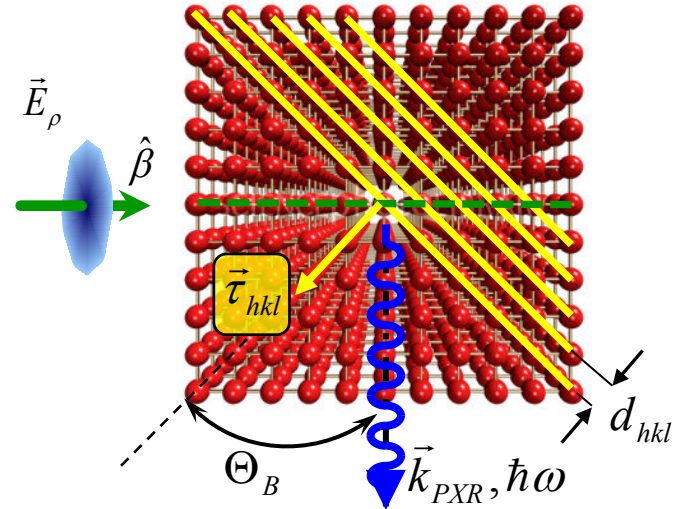


excellent agreement

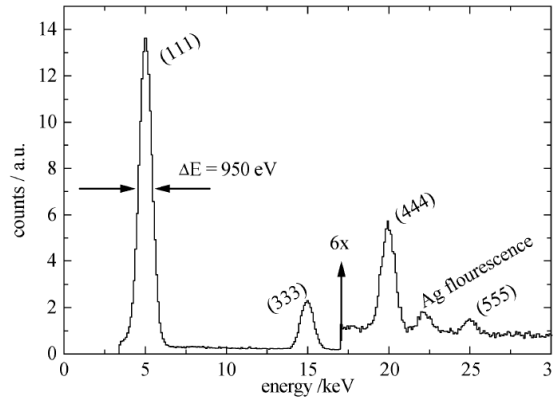
Parametric X-Ray Radiation (PXR)

- **idea:** higher photon energies $\hbar\omega$
 - ▷ better resolution
 - ▷ insensitive on coherent effects
- **real photons**
 - ▷ X-rays \leftrightarrow Bragg reflection, crystals
- **virtual photons**
 - ▷ field separation by Bragg reflection at crystal lattice
 - radiation field: **Parametric X-Ray Radiation (PXR)**
- **crystal periodicity (3D)**
 - ▷ discrete momentum transfer (reciprocal lattice vector $\vec{\tau}_{hkl}$)
 - emission of line spectrum

courtesy: M.J. Winter
 (Science Photo Library)



$$\sin \Theta_B = \frac{\lambda}{2 d_{hkl}}$$



Si crystal
 $E = 855 \text{ MeV}$
 $\Theta_B = 22.5^\circ$
 K.H. Brenzinger et al.,
 Z. Phys. A 358 (1997) 107

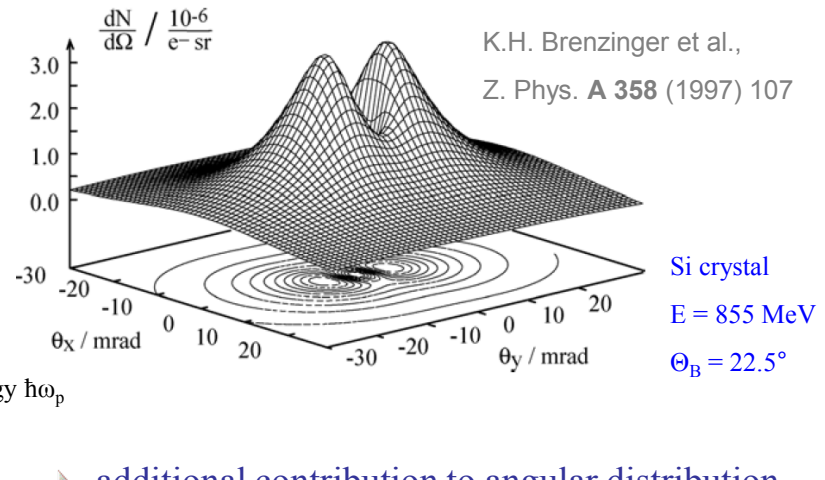
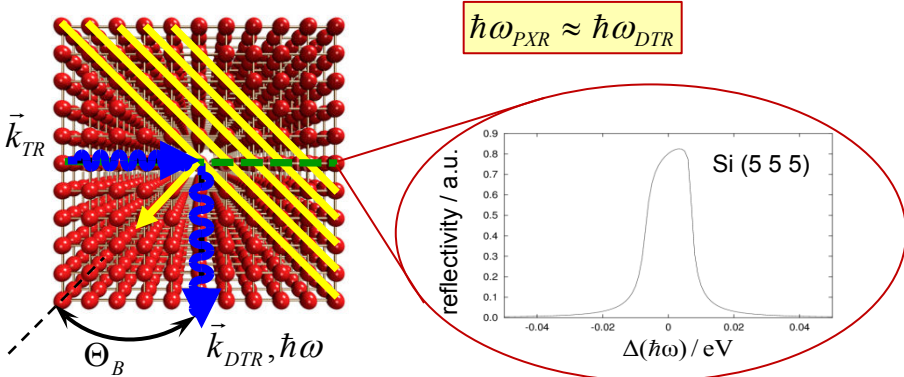
$$\hbar\omega_{hkl} = \hbar c \frac{|\vec{\beta} \cdot \vec{\tau}_{hkl}|}{1 - \sqrt{\epsilon} \vec{\beta} \cdot \hat{k}}$$

$$\epsilon = 1 - |\chi_0|$$

dielectric constant (≈ 1)

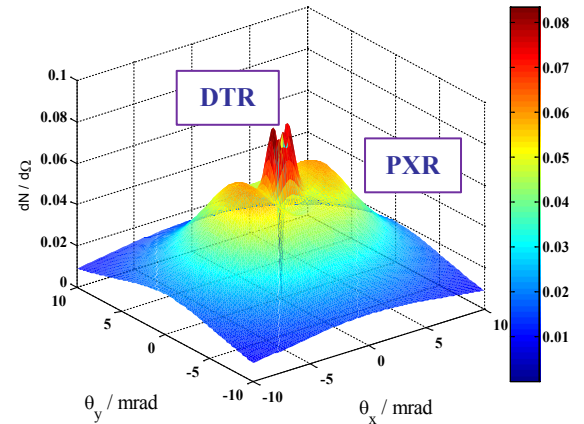
Parametric X-Ray Radiation (PXR)

- **PXR:** Bragg scattering of virtual photons
 - ▶ virtual photon properties retained
 - double lobe angular distribution
- **radiation generation inside crystal**
 - ▶ material properties influence radiation characteristics
 - angular width:
$$\Delta\theta = \sqrt{\left(\frac{1}{\gamma}\right)^2 + \left(\frac{\hbar\omega_p}{\hbar\omega}\right)^2}$$
- **background contribution: real photon diffraction**
 - ▶ transition radiation from crystal entrance surface
 - diffracted at crystal planes under same Bragg angle



- ▶ additional contribution to angular distribution

→ DTR: smaller angular width



A. Caticha, Phys. Rev. A 40 (1989) 4322

radiation amplitude:
$$A_r = A_{c\tau} + R_A(A_v - A_{c0})$$

PXR for Beam Profile Diagnostics

advantage of PXR diagnostics

- › spatial separation from COTR background
 - OTR reflection wrt. surface normal
 - PXR reflection wrt. reciprocal lattice

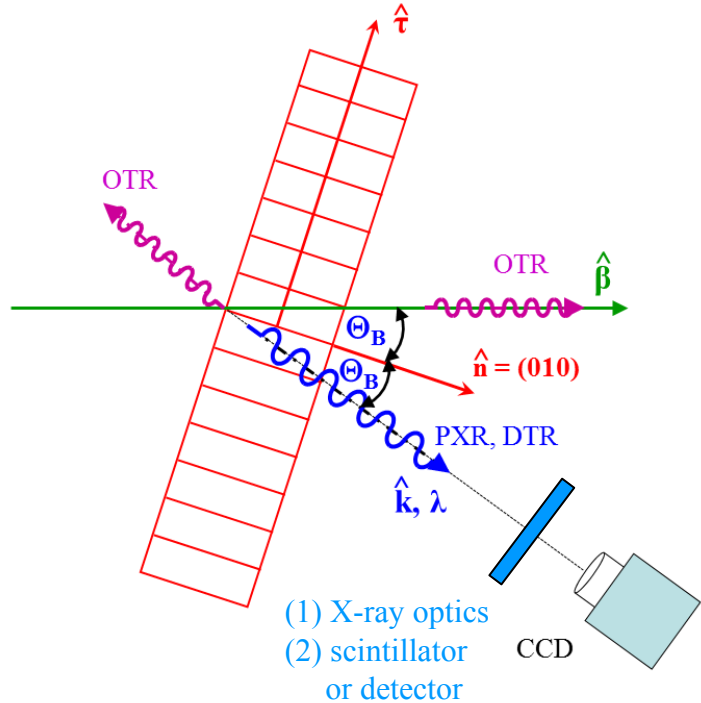
\hat{n}
 $\hat{\tau}$

proposals

- A. Gogolev et al., J. Phys.: Conf. Series **357** (2012) 012018
Y. Takabayashi, Phys. Lett. **A 376** (2012) 2408

detection scheme (1)

- › imaging with X-ray optics
 - sensitivity ?



detection scheme (2)

- › X-ray scintillator/detector close to emission point
 - conversion of X-rays to visible light
 - allows usage of standard optics and CCD
 - parallel object and image plane
 - sensitivity, background ?

detection scheme (3)

- › exploit angular distribution
 - requires exact knowledge of shape
 - PXR / DTR interference, ...
 - additional background contributions ?

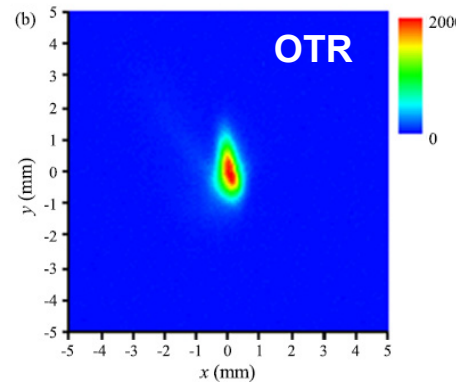
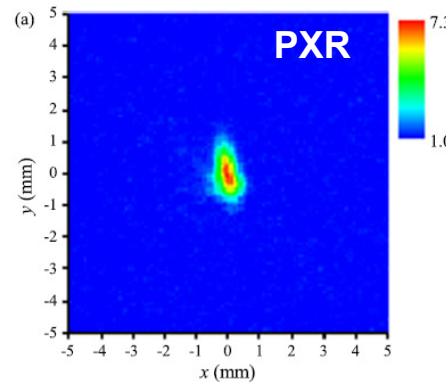
PXR for Beam Profile Diagnostics

direct imaging with pinhole camera

Y. Takabayashi and K. Sumitani, Phys. Lett. A 377 (2013) 2577

test experiment at SAGA Light Source (Japan)

- 255 MeV linac beam, $f_{\text{rep}} = 1 \text{ Hz}$, $I_{\text{avg}} = 7 \text{ nA}$
- Si crystal, $t = 20 \mu\text{m}$, (220) reflection @ 11.6 keV



OTR beam profile

PXR beam profile

- single shot
 - 12600 shots
 - 3.5 h exposure time
- image plate as detector

detector close to emission point

test experiment @ SAGA

Y. Takabayashi, Phys. Lett. A 376 (2012) 2408

- image plate 55.6 mm from target crystal
- 1 sec exposure time
- image plate inside vacuum chamber
- large background contribution

test experiment @ MAMI (Mainz, Germany)

G. Kube et al., Proc. IPAC 2013, Shanghai, China, p.491

- scintillator close to target + CCD
- sensitivity to low, no beam image

PXR Angular Distribution

angular distribution measurements

G. Kube et al., Proc. IPAC 2013, Shanghai, China, p.491

test experiment @ MAMI (Mainz, Germany)

- 855 MeV, $I_{\text{avg}} = 500 \text{ nA}$
 - use of low-cost X-ray CCD
 - (100)-cut Si-crystal, $t = 50 \mu\text{m}$
- $\hbar\omega(220) = 16.55 \text{ keV}$ $\hbar\omega(400) = 23.40 \text{ keV}$

- two (out of 6) beam configurations

Config 1: $\sigma_x = 45.7 \mu\text{m}$ Config 2: $\sigma_x = 44.7 \mu\text{m}$
 $\sigma_y = 42.9 \mu\text{m}$ $\sigma_y = 796 \mu\text{m}$

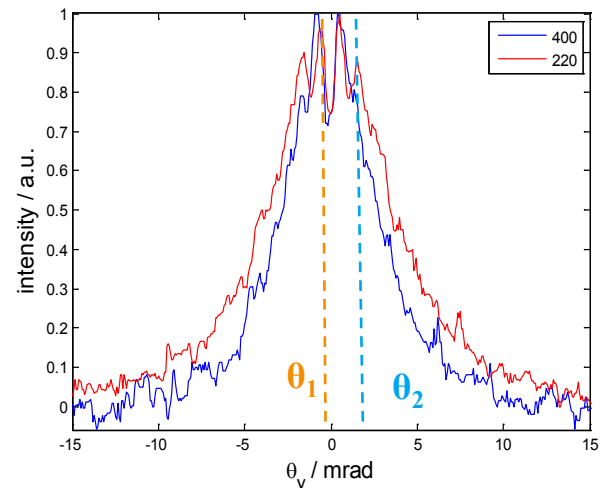
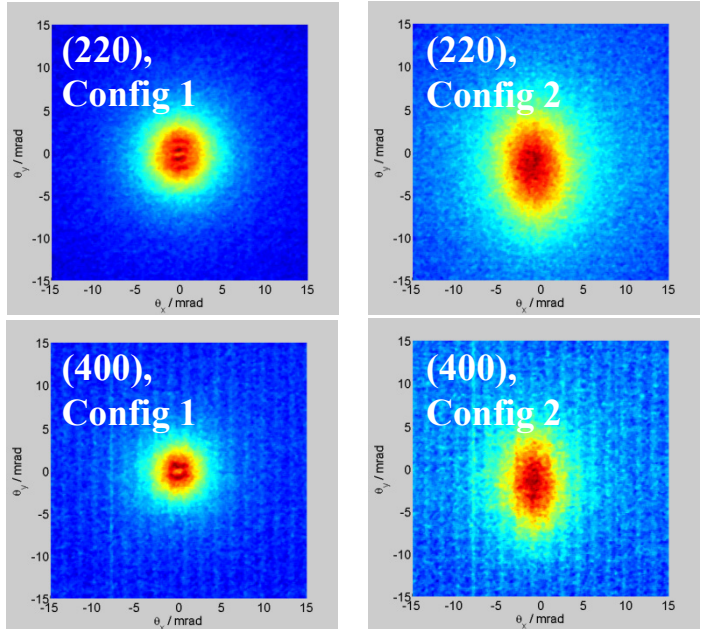
→ angular distribution sensitive on beam size

observation

- θ_1 independent on photon energy: $\theta_1 = 0.6 \text{ mrad} \approx 1/\gamma$
- additional lobes at $\theta_2 \sim 1.8 \text{ mrad}$

interpretation

- significant DTR contribution
- additional contribution from diffracted bremsstrahlung ???



Longitudinal Profile Diagnostics

• Coherent Radiation Diagnostics (CRD)

- standard method for radiation based bunch length diagnostics

O. Grimm, Proc. PAC 2007, Albuquerque, USA, p.2653

• basic procedure

- principle:** bunch length/shape dependent emission spectrum of coherent radiation

$$\frac{dU}{d\lambda} = \left(\frac{dU}{d\lambda} \right)_1 \left(N + N(N-1) |F(\lambda)|^2 \right)$$

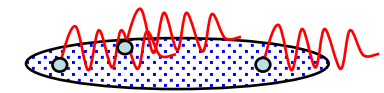
no. of particles per bunch

with

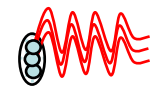
$$F(\lambda) = \int_{-\infty}^{+\infty} dz S(z) e^{-i \frac{2\pi z}{\lambda}}$$

bunch profile

long bunch ($\lambda < \sigma_z$)



short bunch ($\lambda > \sigma_z$)



- measure radiation intensity as function of wavelength in spectral region of interest
 - bunch length determination requires spectral decomposition of intensity
 - intensity-interferometer in THz region (Michelson or Martin-Puplett interferometer)
- Fourier transform
 - **bunch profile and bunch length**
- radiation generation
 - coherent radiation source: synchrotron radiation, transition radiation, diffraction radiation, Smith-Purcell radiation, Cherenkov radiation, ...

Coherent Radiation Diagnostics

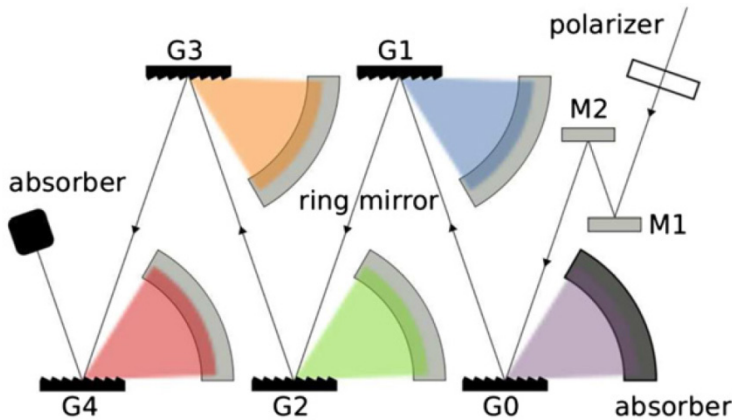
• TR, DR or SR based CRD

- polychromatic emission spectrum
 - spectrometer required for spectral decomposition
- Michelson / Murtin-Puplett interferometers: scanning devices
 - no single-shot capability

• single-shot CRD

- extension to multi-stage single-shot grating spectrometer

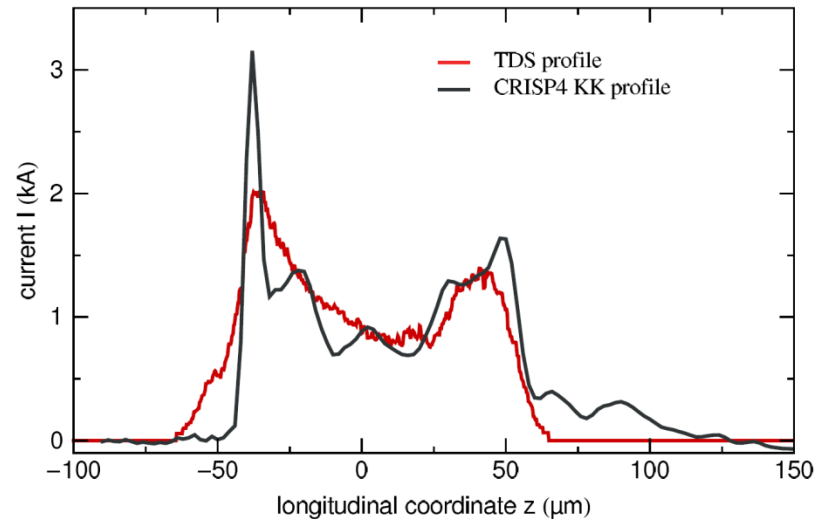
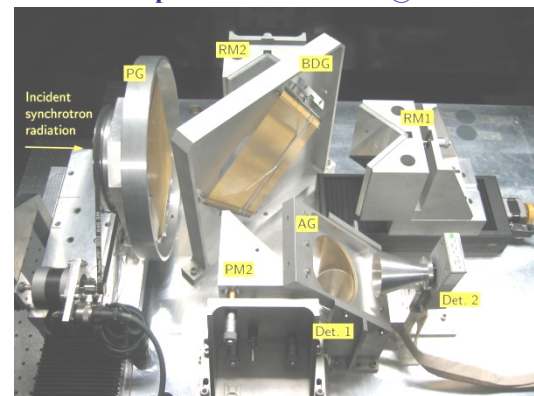
S. Wesch et al., Nucl. Instrum. Meth. **A665** (2011) 40



pyro-electric line detector

30 channels @ room temperature
no window, works in vacuum
fast read out
sensitivity ~ 300 pJ (S/N=5)

Martin-Puplett interferometer @ FLASH



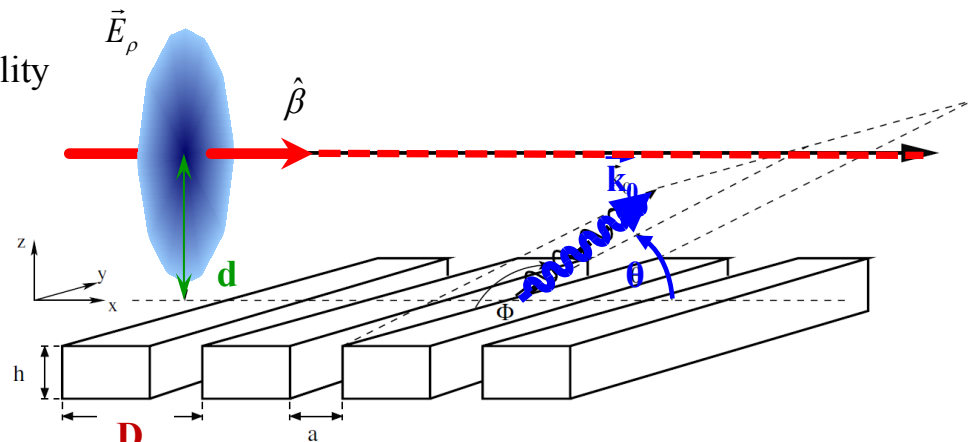
S. Wesch et al., Proc. BIW'12, Newport News (VA), USA, p.256

Smith-Purcell Radiation

- idea: dispersive radiation generation
 - radiation generation and analysis with one device
 - compact setup, option for single-shot capability

Smith-Purcell radiation (SPR)

- field separation
 - virtual photon diffraction at 1D
 - Bravais-structure (grating)
 - grating provides 1D discrete momentum



momentum conservation:

$$\vec{p}_i = \vec{p}_f + \hbar \vec{k} + \hbar n \frac{2\pi}{D} \hat{\mathbf{v}}$$

$$(\vec{p}_i - \vec{p}_f) \cdot \hat{\mathbf{v}} = \hbar \omega = \hbar \vec{k} \cdot \hat{\mathbf{v}} + \hbar n \frac{2\pi}{D} \hat{\mathbf{v}} \cdot \hat{\mathbf{v}}$$

$$2\pi \frac{c}{\lambda} = \frac{2\pi}{\lambda} v \cos \theta + n \frac{2\pi}{D} v$$

$$n\lambda = D \left(\frac{1}{\beta} - \cos \theta \right)$$

→ SPR dispersion relation

distance dependence

→ range of el. field: $\lambda \beta \gamma / 2\pi$

2D field description: $\vec{E} \propto e^{-\frac{2\pi}{\lambda \beta \gamma} d}$

intensity scaling: $I \propto |\vec{E}|^2 \propto e^{-\frac{4\pi}{\lambda \beta \gamma} d}$

SPR identification

→ dispersion relation: necessary condition

→ distance dependence: sufficient condition

SPR for Bunch Length Diagnostics

• proposals

M.C. Lampel, Nucl. Instrum. Meth. **A 385** (1997) 19

D. Nguyen, Nucl. Instrum. Meth **A 393** (1997) 514



dispersion relation: \rightarrow convert angle θ to wavelength λ

• bunch length monitor based on SPR

G. Doucas et al., Phys. Rev. ST Accel. Beams **9** (2006) 092801

V. Blackmore et al., Phys. Rev. ST Accel. Beams **12** (2009) 032803

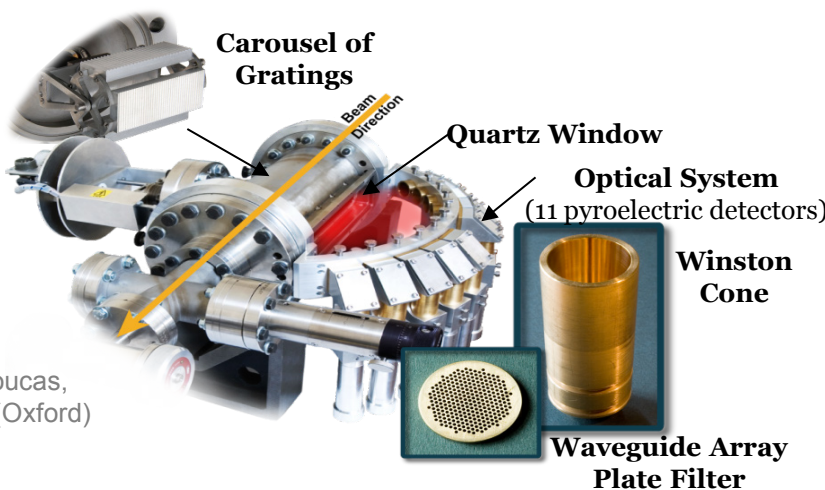
H.L. Andrews et al., Phys. Rev. ST Accel. Beams **17** (2014) 052802

@ **45 MeV** (FELIX)

@ **28.5 GeV** (SLAC, ESA)

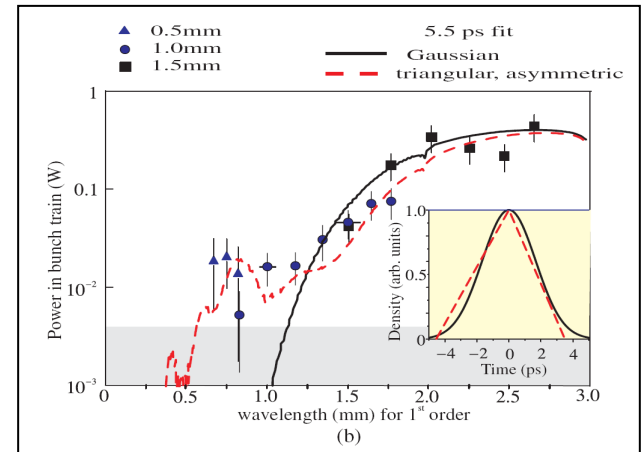
@ **20.35 GeV** (SLAC, FACET)

similar
setup



courtesy G. Doucas,
V. Blackmore (Oxford)

measurement at 45 MeV, FELIX



• critical items

- limited number of points for reconstruction
- single photon emission spectrum

- interferometer: typically about 200 points
- different model predictions, especially at high γ

D.V. Karlovets and A.P. Potylitsyn, Phys. Rev. ST Accel. Beams **9** (2006) 080701

Summary

- **radiation physics widely used for beam diagnostics**
 - longitudinal and transverse beam profiles
 - beam divergence, beam energy, ...
- **circular accelerators: synchrotron radiation**
 - new 3rd generation light sources with ultra-small beam sizes
 - X-ray imaging: possibility to measure beam sizes down to μm level
- **linear accelerators: working horse OTR (+ screens), ODR in experimental stage**
 - OTR: invasive measurement, usually resolution of about $10 \mu\text{m}$
 - better resolution → smaller wavelengths (EUV), PSF-dominated imaging
 - new 4th generation light sources → coherent emission compromises use of OTR as reliable diagnostics
 - ODR: high resolution measurements via angular distribution → ODRI offers possibility to resolve ambiguities
- **PXR: interesting for X-ray region**
 - still in early experimental stage → first experiments in view of beam diagnostics
- **CRD: bunch length/shape measurements**
 - CTR, CDR, CSR → spectral decomposition with interferometers
 - CSPR → dispersive emission characteristic, but still some open questions...

Outlook

• commercial codes applied to radiation physics

- TR generation with CST Particle Studio®

K. Lekomtsev et al., Journal of Physics: Conference Series **517** (2014) 012016

- OTR/ODR generation and propagation with ZEMAX®

T. Aumeyr et al., Proc. IBIC 2013, Oxford, UK, p.852

T. Aumeyr et al., Journal of Physics: Conference Series **517** (2014) 012026

T. Aumeyr et al., Proc. IPAC 2014, Dresden, Germany, p.3722

• (Surface) Cherenkov Radiation

- growing interest
 - as radiation source
 - but also for beam diagnostics

A.S. Konkov et al., Journal of Physics: Conference Series **517** (2014) 012003 ...

• Acknowledgment

- for the invitation to this conference and the opportunity to give a talk
- for stimulating discussions and help in preparation of this talk
 - A. Cianchi (INFN and Univ. Rome), P. Karataev (RHUL), D. Nölle (DESY),
 - A.P. Potylitsyn (TPU), N.A. Potylitsina-Kube (DESY), K. Wittenburg (DESY)
- for your attention